THE JOURNAL OF PHYSICAL CHEMISTRY C

Article

pubs.acs.org/JPCC

Probing Charge States in Molecular Junctions Using Raman Spectroscopy

Fatemeh Mirjani,*[,†] Joseph M. Thijssen,[†] and Mark A. Ratner[‡]

[†]Kavli Institute of Nanoscience, Delft University of Technology, Lorentzweg 1, 2628 CJ Delft, The Netherlands

[‡]Department of Chemistry, Northwestern University, 2145 Sheridan Road, Evanston, Illinois, 60208-3113, United States

ABSTRACT: We examine the Raman spectra of a series of molecules in different charge states and suggest ways of controlling these charge states in charge transport experiments. Our study uses density functional theory (DFT)-based quantum chemical methods. The molecules we study are benzene derivatives, which accommodate transport either through the HOMO or the LUMO (where the HOMO and the LUMO denote the highest occupied molecular orbital and lowest unoccupied molecular orbital, respectively). We have investigated whether observable differences in the Raman spectra will occur upon electron addition or removal. We find substantial frequency shifts upon electron removal or addition. These shifts tend to be uniformly downward in the case of LUMO transport, whereas, for HOMO transport, this unidirectionality is lacking and it is due to the fact that anions are usually less strongly bound than neutrals, whereas removing an electron from a bonding-type orbital usually gives localized modification in bond length and strength.

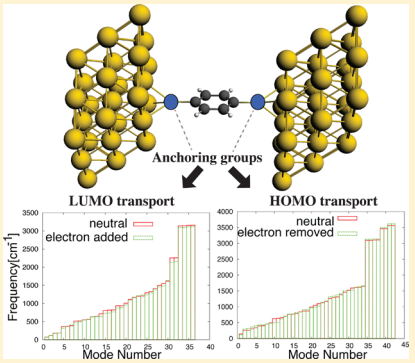

INTRODUCTION

The field of molecular electronics is based on the idea that molecules can be used to construct nanodevices exhibiting novel functionality.[1−3] Scanning tunneling microscopy (STM) can be used to visualize molecules on metallic surfaces or for current−voltage spectroscopy (in which the tip is not moved).[4−6] For independent and simultaneous characterization of the current−voltage signal and the molecular structure, spectroscopic tools, in combination with charge transport junctions, seem appropriate. Raman spectroscopy can give insight into the vibrational spectra, and therefore into the mechanics of the molecule. The problem with this spectroscopic technique is that Raman scattering from a single molecule is not detectable for common field intensities. However, a pleasing feature of Raman spectroscopy for molecular junctions is that the field is strongly enhanced in narrow gaps between two gold surfaces (on average by a factor of 10^5−10^6 and sometimes even by a factor of 10^{14}−10^{15}).[7−14] This phenomenon is known as surface-enhanced Raman spectroscopy (SERS); it was observed by Fleischmann[15] and explained by Jeanmaire and Van Duyne.[16] SERS enables the detection of Raman signals from a single molecule on a metallic surface. Consequently, if signals can be seen in molecular junction experiments, they can be attributed mainly to the molecules that are trapped in between the metallic electrodes.

A few studies in this direction have appeared.[17−23] For instance, Ward et al. carried out simultaneous measurements of conductance and Raman spectroscopy in a junction made by electromigration.[17] Their results show that the Raman response of both *p*-mercaptoaniline and a fluorinated oligophenylyne ethynylene correlates in time with changes in the electronic conductance. These results suggest that the observed changes in the Raman spectrum and the conductance are due to the changes in the conformation and binding of individual molecules. Tian et al. used SERS with a mechanically controlled break junction for 1,4-benzenedithiol and demonstrated enhancement of Raman intensities upon the reduction of gap width.[24] More recently, Liu et al. showed simultaneous measurements of the tip-enhanced Raman spectroscopy and molecular conductance by STM in room temperature.[19] They showed that Raman spectroscopy can be related to the molecular structure in the junction. In their experiment, the electromagnetic field is enhanced by the presence of the gold tip and the substrate, and it is shown that, as the molecule is trapped between the metal substrate and the tip, the Raman scattering increases substantially while the contribution from molecules outside the junction is not significant. In addition, they studied the Raman spectrum for different bias voltages and observed a voltage-dependent peak splitting (of the order of 22 cm^{-1}) which was explained in terms of different bonding interactions between the gold tip/substrate and the molecule.

METHOD

In this paper, we calculate Raman spectra for different charge states of several molecules, anticipating experiments in this direction.

If the molecule is strongly coupled to the electrodes, its charge is usually fractional and fluctuates only a little. In the opposite limit, where the molecule is weakly coupled to the electrodes, the passage of an electron from one electrode to

Received: August 3, 2012
Revised: October 8, 2012
Published: October 10, 2012

dx.doi.org/10.1021/jp307703t | *J. Phys. Chem. C* 2012, 116, 23120−23129

another one occurs sequentially via a charged state of the molecule. This regime, often denoted as the Coulomb blockade regime, is characterized by integer charge transfer, and possibly substantial fluctuation. In this paper, we focus on this weak coupling regime and compare the vibrational modes and Raman intensities of neutral molecules with those of molecules with one electron added or removed.

The most convenient way of changing the charge state is by using a weakly coupled three-terminal junction, in which a gate voltage can be used to push levels across the Fermi level of the contacts.[25−27] The large majority of experimental setups use a two-terminal geometry. To be able to change the charge states in such a setup, the tunnel couplings to the leads should be much smaller than the level splitting of the molecule inside the junction. These couplings denoted by $\Gamma_k (k = \mathrm{L}, \mathrm{R})$ should also be small enough that the dwell time of an electron (which is of the order of $\hbar/\Gamma$) is longer by an order of magnitude than the period of the normal mode under study. For a typical weak coupling value of 10 meV, this means that the normal-mode frequencies should be at least 100 meV (806 cm^{-1}).

It is important to distinguish between the tunnel and the capacitive couplings. These are correlated but different quantities: the first determines how easily an electron can flow through the contact region, and the second determines the location of the orbital levels with respect to the Fermi levels of the two contacts. All in all, two scenarios are possible in the weak coupling limit for a two-terminal device in the transport (i.e., non-blockaded) regime: (i) the charge fluctuates between two values, and each of these values is maintained for a relatively long time (long in the sense discussed in the previous paragraph), and (ii) the charge takes on one value only for nearly all the time. The second case requires strongly asymmetric tunnel couplings. It is interesting to see whether, in that case, the charge state can be influenced by the bias voltage. This is possible, unless the strong asymmetry in the tunnel coupling is reflected in the capacitive coupling: if both the tunneling and capacitive couplings are much stronger for one lead than for the other, the location of an orbital with respect to the Fermi energy of that lead determines the charge state. This situation typically occurs in many STM experiments in which the tip couples much more weakly (in the capacitive and tunneling sense) to the molecule than the surface: then the charge state cannot be changed, as is fully determined by the substrate.

In order to have more than one well-defined charge state on a molecule, comparable capacitive and highly asymmetric tunnel couplings are both required. The mechanism is shown in Figure 1.

We conclude that, in the case of weak tunnel coupling and comparable capacitive couplings, two scenarios can occur: the charge will every now and then flip from one value to another, or there is only one charge state most of the time, and this state can be triggered by the bias voltage. These scenarios will give the following Raman features. The first case (flipping between two charge states) will result in a superposition of the Raman spectra of the two charge states. The second case will give a Raman spectrum which will change when the bias voltage crosses a value where the charge state of the molecules is changed. It is important to note that, apart from these abrupt changes, there is a gradual change in the spectrum due to the Stark shift induced by the bias voltage.[28]

In Figure 1, a non-symmetrically coupled molecule is considered, in which transport takes place through the

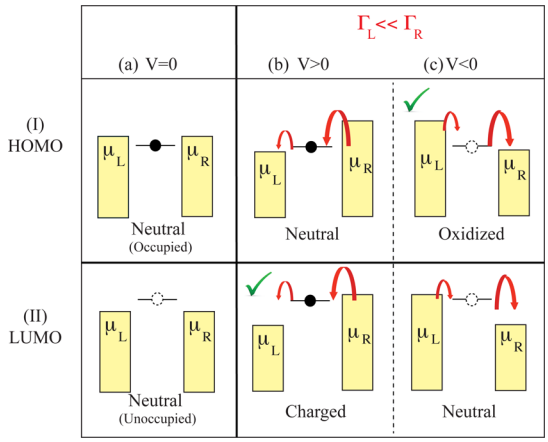

Figure 1. The transport through a molecular (I) HOMO or (II) LUMO level in the case of zero bias and nonzero bias. The size of the tunnel coupling is indicated by the width of the red arrows: the left coupling is considered to be weaker than the right coupling: $\Gamma_L \ll \Gamma_R$ (although Γ_R should still be much smaller than the level spacing). We assume that the capacitive couplings are equal: the chemical potentials of the electrodes for the positive biases are $\mu_{L,R} = E_F \mp V/2$ and for the negative biases are $\mu_{L,R} = E_F \pm V/2$. In the cases which are shown by green ticks, the molecular level can remain charged or oxidized for a significant amount of time due to the asymmetric couplings. For instance, if the transport is through the HOMO and the applied bias is negative (upper left panel), due to the much stronger coupling to the right electrode, the molecule can easily lose an electron. Due to the weak coupling to the left electrode, it remains in an oxidized state for a substantial amount of time. However, in the case of positive bias voltage, as the left coupling is weaker than the right coupling, the molecule does not lose its electron very fast. If the transport is through the LUMO, by applying a positive bias voltage (midbottom panel), the charge flows from the right electrode into the LUMO and it remains there for a substantial amount of time. However, if the applied bias voltage is negative, the electron which jumps from the left electrode to the molecule goes to the right electrode immediately, since the right coupling is much stronger than the left coupling.

LUMO (where LUMO denotes the lowest unoccupied molecular orbital) and where the left coupling is much smaller than the right coupling ($\Gamma_L \ll \Gamma_R$), although Γ_R should still be much smaller than the level spacing. By applying a positive bias voltage, the charge flows from the right electrode into the LUMO and it remains there for a substantial amount of time. However, if the applied bias voltage is negative, the electron which jumps from the left electrode to the molecule goes to the right electrode immediately, since the right coupling is much stronger than the left coupling. Similar mechanisms can occur when the dominant level in the transport is the HOMO (where HOMO denotes the highest occupied molecular orbital), as shown in Figure 1. In this case, if the applied bias is negative, due to the stronger coupling to the right electrode, the molecule can lose an electron and, due to the weaker coupling to the left electrode, it remains in an oxidized state for a substantial amount of time. However, in the case of positive bias voltage, as the left coupling is weaker than the right coupling, the molecule does not lose its electron very fast.

There are two ways to create a molecular junction with asymmetric tunnel couplings. The first one is using different electrode materials, which is possible in a STM setup in which the coupling of the molecule to the metallic surface is generally much higher than to the tip. Another way is using an asymmetric molecule. Finally, molecules often happen to bind

dx.doi.org/10.1021/jp307703t | J. Phys. Chem. C 2012, 116, 23120−23129

more strongly to one electrode than the other, due to particular circumstances, such as asymmetric electrodes, or random steps in the junction formation process. Depending on whether the transport in a molecule is through the LUMO or the HOMO, the electrons will be added to or removed from the molecule during current flow.

In order to allow for the detection of bias-induced charging in experiments, we study the difference between the Raman spectra of different charged states, and verify whether charge-induced structural changes lead to observable changes in the Raman spectra.

RESULTS AND DISCUSSION

We now present the results of vibrational mode analysis and Raman spectra for the six molecules shown in Figure 2.

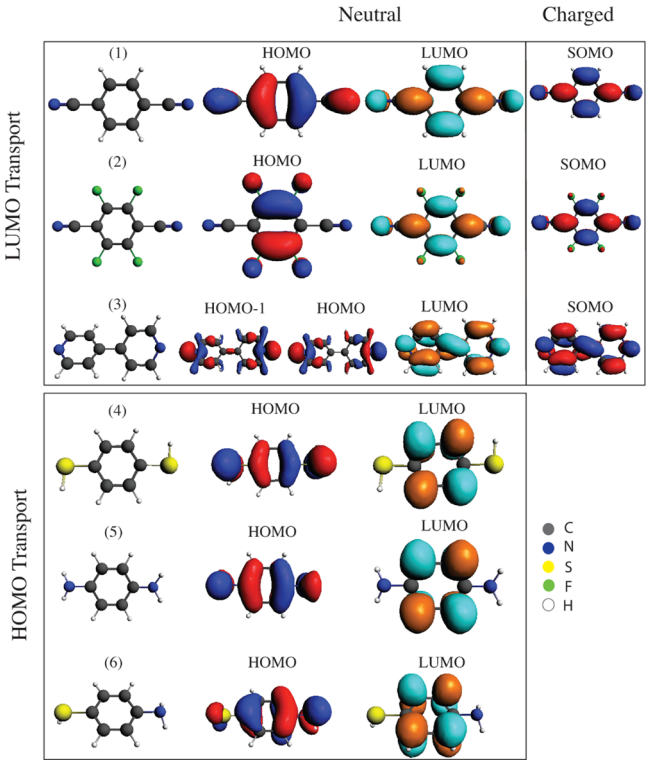

Figure 2. The structure, the HOMO, and the LUMO of *neutral* molecules and the SOMO (singly occupied molecular orbital) of *charged* molecules (after adding an electron). The gray, blue, yellow, green, and white atoms present carbon, nitrogen, sulfur, fluorine, and hydrogen atoms, respectively. The transport through the first three molecules is through the LUMO, and it is through the HOMO in the last three molecules. The SOMOs of charged molecules 1, 2, and 3 are similar to the LUMOs of neutral ones. (1) Molecule 1: 1,4-dicyanobenzene: A benzene ring with two cyano groups. (2) Molecule 2: 1,2,4,5-tetrafluoro-3,6-dicyano-benzene: Tetrafluorobenzene with two cyano linkers. (3) Molecule 3: 4,4′-Bipyridine in which two benzene rings are known to be twisted.[39,53,54] The HOMO and the HOMO-1 are nearly degenerate in this molecule. (4) Molecule 4: 1,4-benzenedithiol: A benzene ring with two thiol linkers. (5) Molecule 5: 1,4-diaminobenzene: A benzene ring with two amine linkers. (6) Molecule 6: *p*-mercaptoaniline: A benzene ring with one thiol linker and one amine linker. The observation that in molecules 1 and 2 the transport is through the LUMO while in molecules 4−6 it is through the HOMO is suggested by substituent trends (electron withdrawing and electron donating) of physical organic chemistry.[55]

After doing the geometry optimization, for the neutral and charged states, we perform the vibrational modes analysis. All Raman calculations are done using density functional theory (DFT), within the Q-Chem program with a 6-31G** basis set and the PBE exchange-correlation functional.[29] The Raman effect is sensitive to the electron−vibron coupling, which determines the intensity of the observed spectral lines. The Raman intensity calculation begins with the determination of the harmonic frequencies and normal coordinates of vibrations. To compute these, the Hessian matrix (the second derivative of energy with respect to the nuclear position) is calculated. The mass-weighted Hessian matrix is then diagonalized, yielding the vibrational frequencies, and the eigenvectors which define the normal coordinates and therefore the changes in polarizability. The polarizability calculations are performed for geometries that are displaced from equilibrium along the normal coordinates, so that the Raman intensities can be calculated.[30]

In our vibrational analysis calculations, we neglect the effects of the nearby electrodes, since we discuss the weak coupling regime. To check whether screening effects of the nearby gold influence the Raman spectrum, we have performed constrained DFT (CDFT) calculations (within the Q-Chem program[29]) in which the charge is constrained on the molecule in the presence of gold electrodes. These calculations yield results similar to those obtained for isolated molecules without any gold electrode. Moreover, our calculation agrees with the Raman spectrum of 4,4′-bipyridine as measured by Liu et al.[19] in simultaneous measurements of Raman spectroscopy and molecular conductance (see Figure 3A).

To check whether constraints due to the anchoring groups of the molecule shift the spectrum, we have considered 1,4-benzenedithiol which was used by Tian et al. with a mechanically controlled break junction.[24] Our result is similar to their experimental spectra (see Figure 3B). When the hydrogen atoms of the thiol groups are assigned the mass of a gold atom, we see a similar spectrum to the one for the isolated molecule, as shown in Figure 3C (except for low frequency modes which are not interesting for our purposes as discussed above, for a typical weak coupling value of 10 meV, the normal modes should be at least ∼800 cm^{-1}). The C−H stretch modes, which would be expected to be most sensitive to this substitution, are far to the blue (∼3000 cm^{-1}).[31]

It should be noted that, in general, the SERS modes, which would ordinarily be Raman forbidden by symmetry in the gas phase, may show up in SERS spectra, since interactions with the metal lead to a total polarizability tensor of lower symmetry than just the molecule. In this manuscript, we focus on strongest modes. The Raman intensity of forbidden modes tends to be weak,[32] even more so for the weakly coupled junctions required for observing sudden changes in the molecular charge.

All molecules shown in Figure 2 contain a benzene ring. They differ in the type of the anchoring groups connecting these molecules to the left and right electrodes, and in molecule 2, the four hydrogen atoms of the benzene ring are replaced by the fluorine atoms. The cyano (—C≡N) linkers in molecules 1 and 2 which have been recently used in molecular junctions as new promising anchoring groups[33−36] are electronegative, which means that they push the LUMO closer to the gold Fermi energy.[35] Molecules 1 and 2 in Figure 2 are relatively electronegative, and it is therefore expected that LUMO transport is possible. In molecule 3, which consists of two benzene rings, two carbon atoms are replaced by nitrogen

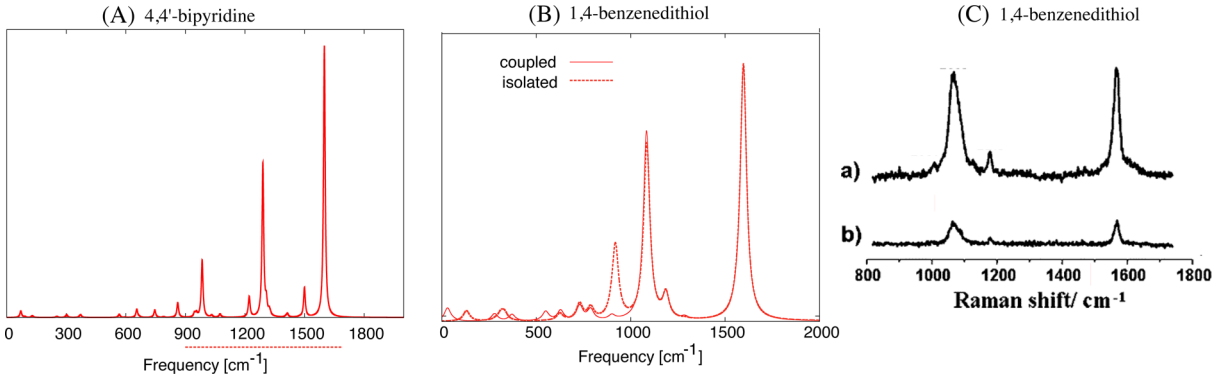

Figure 3. (A) 4,4′-Bipyridine: The calculated Raman spectrum for *isolated* 4,4′-bipyridine. The horizontal dotted line between 900 and 1700 cm^{-1} indicates the frequency range where the spectrum was measured by Liu et al. Our results are in agreement with the results of Liu et al., in the *presence* of gold electrodes.[19] (B) 1,4-Benzenedithiol: When the mass of hydrogen atoms of the anchoring groups is assigned the mass of an Au atom, largely the low frequency modes change compared to the isolated molecule with hydrogen atoms at two ends. The Raman spectrum of 1,4-benzenedithiol is in agreement with the Raman spectrum measured by Tian et al. shown in part C either when the molecule is isolated or when its two ends attached to two hydrogen atoms with the mass of gold atoms. (C) 1,4-Benzenedithiol: (Reprinted with permission from *J. Am. Chem. Soc.* **2006**, *128*, 14748[24]) The reprinted figure is for two cases, where the gold electrode pair has its axis (a) parallel and (b) perpendicular to the incident polarization.

which is more electronegative (this molecule consists of two pyridyl groups (PY)). Also, in this molecule, the transport is expected to be through the LUMO. The simultaneous measurement of Raman spectra and conductance for this molecule was performed by Liu et al. In their experiment, the molecule is strongly coupled to the electrodes.

For the remaining three molecules, hole-like transport (through the HOMO) is expected. Molecules 4 and 5 are the usual, historic testbed molecules for charge transport, benzenedithiol and benzenediamine. To study a molecule with asymmetric coupling to the electrodes, we consider a benzene ring with one thiol linker and one amine linker used by Ward et al. in the simultaneous measurements of conductance and Raman spectroscopy.[17] This molecule is labeled "molecule 6" in Figure 2.

The different anchoring groups used here have different strength and junction formation probability. Recent experiments have revealed the following sequences for (i) junction formation probability and (ii) binding energies of the anchoring groups to the electrodes we have used in this paper:[37] (i) PY > SH > NH_2 > CN; (ii) Au−S ≫ Au−PY > Au−CN > Au−NH_2. The tunnel couplings are expected to follow a similar trend. Indeed, the molecular level broadening (due to tunnel coupling) for the cyano anchoring group is found to be 40% smaller than for the thiol coupling.[34] The amine coupling to the metal is also known to be weaker than the thiol coupling.[38] The coupling as found in experiments varies, however, and particularly in electromigrated junctions, it is often a lot weaker.

In the results presented below, the frequencies are presented in cm^{-1} and the Raman intensities are presented in arbitrary units. In the spectra, the Raman signals of vibrational modes are broadened by a Lorentzian function with a width of 20 cm^{-1}. The heights of Raman peaks are not comparable with the experiment, since the presence of a metallic electrode in the experiment enhances these intensities. However, the relative heights should be similar.

LUMO Transport. *Molecules 1, 2, and 3: Benzene and Tetrafluorobenzene with Two Cyano Linkers, and 4,4′-Bipyridine.* In order to find an indication of whether the LUMO is closer to the Au Fermi energy than the HOMO, we have performed transmission calculations on the basis of the nonequilibrium Green function (NEGF) approach. Although this approach reflects the characterization of molecules in the strong coupling regime and is known to suffer from a few problems, mainly related to its inability to correctly describe energy gaps and level alignments of molecules at surfaces, it can be used in the weak coupling regime to give an indication whether the transport is electron-like (LUMO) transport or hole-like (HOMO) for the following reasons:

(i) Our results match with known experimental results (except for molecule 2 for which no experimental results are available).[36,39−44] (ii) Strange et al.[45] have shown that, although the conductance predicted by NEGF is not correct, this method can predict HOMO or LUMO transport correctly. (iii) The so-called scissors operator has been used in ref 46 to correct for the self-interaction error and image charge effect. These calculations agree with our NEGF calculations on the point whether transport is through the HOMO or LUMO.[46]

We start by presenting the results of NEGF calculations for molecules 1 and 2. The code used here is an in-house developed add-on to the Amsterdam density functional (ADF) code (using an LDA exchange correlation functional and a double-ζ polarized basis set) based on a Hamiltonian with converged zero-bias junctions with finite-sized contacts.[47] The structure of the extended molecule 1 connected to the electrodes is shown in Figure 4.

The transmission results are presented in Figure 5. Molecules 1 and 2 contain cyano groups (nitrile) which are electronegative.[33,35] For molecule 1, both experiment[36] and theoretical

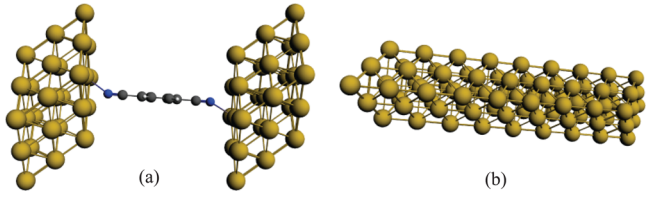

Figure 4. (a) Geometry of the extended molecule used in the transport calculation for molecule 1. (b) Geometry of the electrode used in the calculation of the self-energies which consists of nine layers of nine atoms each.

dx.doi.org/10.1021/jp307703t | J. Phys. Chem. C 2012, 116, 23120−23129

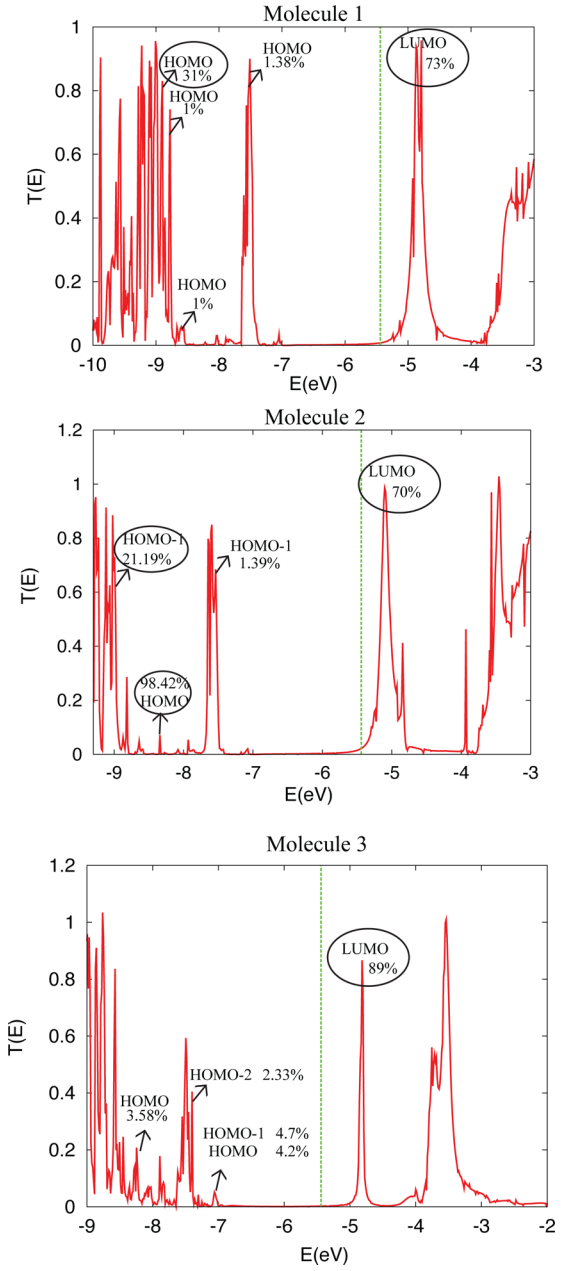

Figure 5. The transmission for molecules 1, 2, and 3. The vertical dashed lines show the Fermi energy at −5.44 eV. In all molecules, the LUMO is closer to the Fermi energy than the HOMO. The percentage of the HOMO/LUMO contribution in each transmission peak is shown. The peaks shown by circles present the major contributions. There are some peaks with a small contribution of HOMO/HOMO-1, due to the fact that the transport orbitals in the presence of the leads do not match the orbitals of the isolated molecule exactly.

calculations[48] suggest that the transport is dominated by the LUMO. Our calculations confirm this. The Fermi energy of the gold electrode in our calculation is −5.44 eV, chosen to be in the middle of the HOMO−LUMO gap of the electrode (the gold electrode model consists of nine layers of nine atoms each). For molecule 1, as shown in Figure 5, the LUMO peak is much closer to the Au Fermi energy than the HOMO. The HOMO energy of the isolated molecule is −8.26 eV, and the LUMO energy is −4.14 eV.

In molecule 2, due to the replacement of hydrogen by electronegative fluorine atoms, it is expected to see the LUMO closer to the Au Fermi energy than in molecule 1. For molecule 2, the HOMO and LUMO energies of the isolated molecule are −8.1 and −4.8 eV, respectively. In this molecule, also, the LUMO peak appears close to the Fermi energy in the NEGF calculations. The level shifts in the junction are due to electron transfer. Furthermore, image charge effects will move the HOMO and LUMO closer together.[49] Nevertheless, our calculations suggest that, upon increasing the bias, the LUMO is likely to enter the bias window. Therefore, we explore the difference between the Raman spectra for the neutral molecule and the molecule with one extra electron.

One could also replace one of the cyano groups in molecule 2, by a fluorine atom which provides an asymmetric coupling when it is trapped in the gap between two electrodes. Our transport calculations suggest that such a molecule accommodates transport through the LUMO.

For molecule 3, the calculations for the isolated molecule show that the energy of the LUMO is −3.4 eV and the HOMO and HOMO-1 are essentially degenerate, both with the energy of −6.4 eV. This means that, for the isolated molecule, the LUMO energy is not closer to the Fermi energy than the HOMO. However, our transmission in Figure 5 shows that the transport in molecule 3 is through the LUMO which is in agreement with other theoretical and experimental studies.[39−41] The LUMO energies are not so reliable as the HOMO in DFT calculations, and when occupied, they change their energies (becoming a SOMO). Thus, the idea of LUMO energies is totally a qualitative (or at least semiqualitative) one.

Figure 6 shows a comparison between the vibrational spectra of the neutral and the negatively charged molecules 1, 2, and 3. All frequencies are positive as they should be, indicating that the geometries are well-optimized. There are some modes in which the frequency for the charged molecule is different (lower) from that for the neutral molecule. Most of these lie in the high-frequency range of the spectrum. The frequency of these modes is lowered when the molecule is charged because the extra charge tends to weaken the bonds; i.e., the nuclear charges are screened more strongly by the extra electron and therefore the vibrations become slower.[50]

For molecules 1, 2, and 3, we identify regions in which frequencies vary significantly upon charging the molecule—they are labeled in Figure 6 as A, B, C, D, and E. For molecule 1, the corresponding peaks for these regions are labeled accordingly in the Raman plot in Figure 7. As shown, only the frequencies in region C are shifted upward—in the remaining areas, they are lowered. Not all vibrational modes show separate peaks in the Raman plot due to differences in electron−phonon coupling and because closely spaced frequencies are not always resolved individually. Moreover, not all modes are strongly Raman active. For example, mode 29, for molecule 1, shows a change in frequency upon charging the molecule, but no peak is observed for this mode in the Raman plot due to the small Raman intensity of this mode.

It is important to note that the charge-state-induced frequency shifts that we predict are usually larger than the frequency shifts due to the conformational changes observed in experiments. For instance, in the STM experiment by Liu et al.,[19] the observed frequency shift was 22 cm^{-1}, whereas the frequency shifts that we predict here are of the order of 100 cm^{-1} in regions A and D. The observed peak splitting in the (room temperature) STM experiment by Liu et al.[19] is a voltage

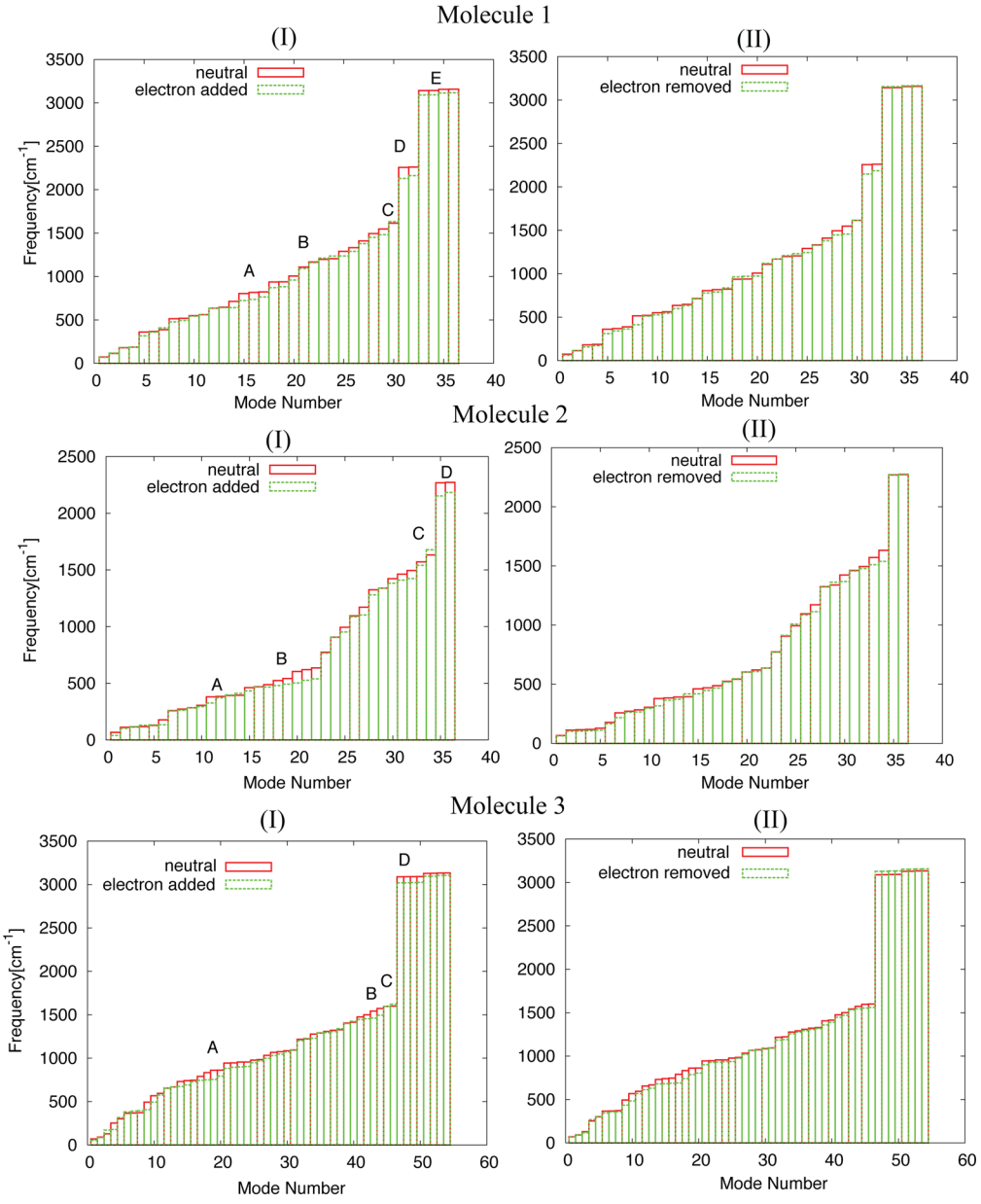

Figure 6. Molecules 1, 2, and 3: (I) The frequencies of all vibrational modes for the neutral molecule and the molecule charged by *adding* an electron. (II) The frequencies of all vibrational modes for the neutral molecule and the molecule with one electron *removed*. The A, B, C, D, and E label the regions where the modes differ significantly between neutral and charged cases.

dependent phenomenon, and since their molecule is strongly coupled to the electrodes (and therefore is partially charged), we infer that this observation is not due to probing of the charged states.

In molecule 2, where the hydrogen atoms are replaced by fluorine, the vibrational spectrum changes in a way similar to molecule 1 upon electron addition. In this case, 36 vibrational modes exist. The regions labeled by A, B, C, and D show significant shifts in their frequencies upon charging the molecule (see Figure 7). All mode frequencies which are changed upon charging the molecule are lowered, except for the mode shown in region C. A similar trend is observed for molecule 3, shown in Figures 6 and 7. For molecules 1, 2, and 3, we also compare the frequencies of the neutral molecule to those of the molecule in which one electron is removed. As shown in plots II of Figure 6, the regular trend observed for adding an electron to the system is not seen when an electron is removed.

The resulting analysis predicts a difference in the Raman spectra which is easier to detect for neutral and negatively charged molecules than for neutral and oxidized molecules.

HOMO Transport. *Molecules 4 and 5: A Benzene Ring with Two Thiol Linkers or Two Amine Linkers.* It is well-known that the transport through a benzene ring with thiol or amine linkers is hole-type, or HOMO transport.[42−44] Our NEGF results for transmission through these molecules are shown in Figure 8; they are in good agreement with other results for these frequently studied molecules.[42−45] For molecule 4, the NEGF calculations are done with the usual sulfur−gold binding with the hydrogen atoms removed. As shown in Figure 8, the HOMO peak is closer to the Fermi energy than the LUMO. For molecule 4, the HOMO and the

dx.doi.org/10.1021/jp307703t | J. Phys. Chem. C 2012, 116, 23120−23129

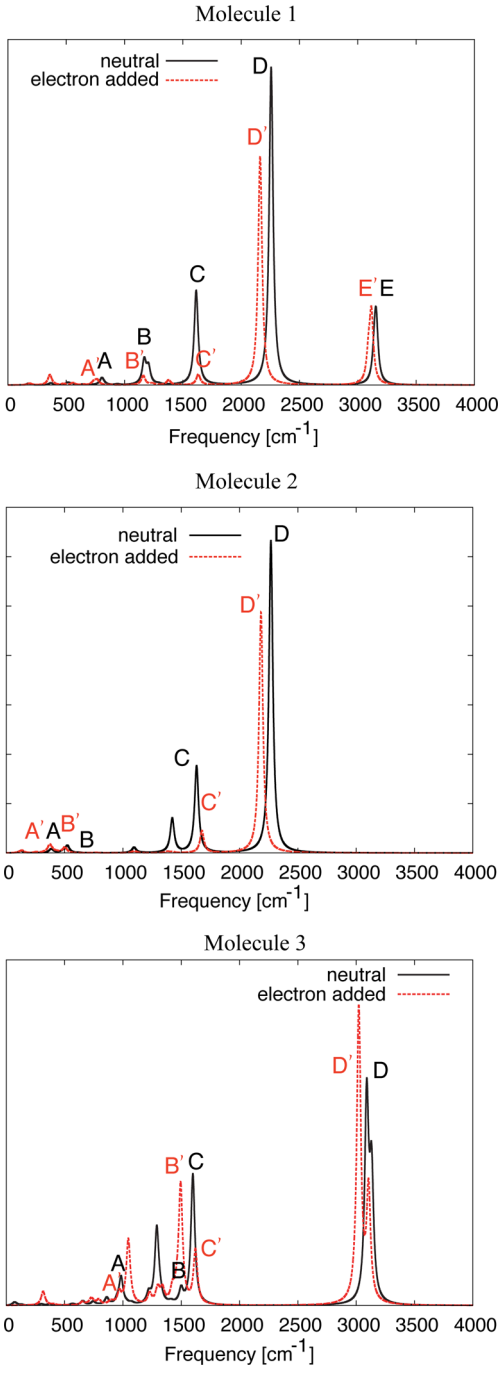

Figure 7. Molecules 1, 2, and 3: The Raman spectrum for the neutral molecule and the molecule charged by *adding* an electron. The peaks in regions A, B, C, D, and E for the neutral molecule are shifted to A', B', C', D', and E' when the molecule is charged.

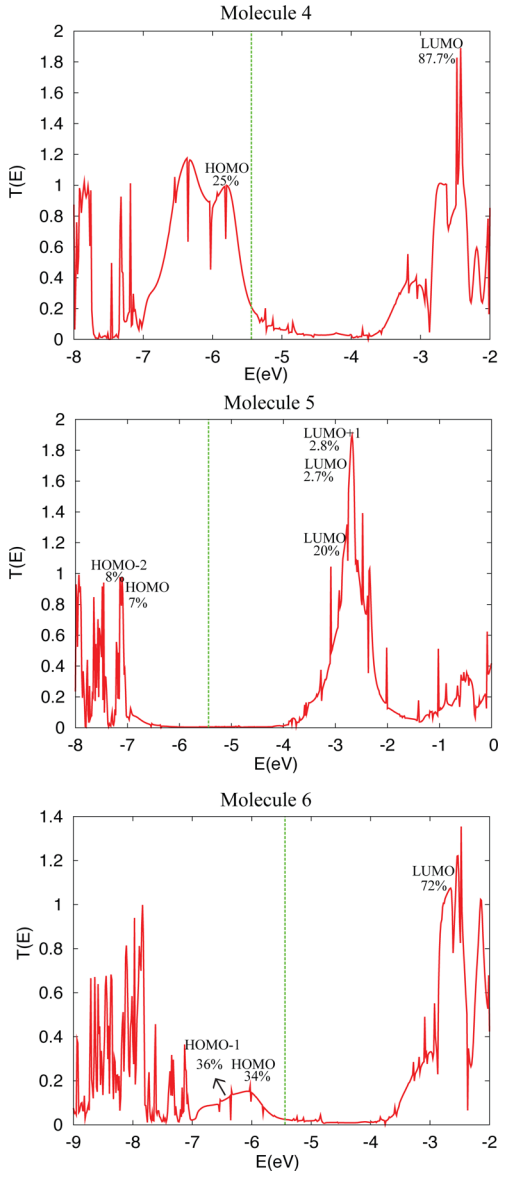

Figure 8. The transmission for molecules 4, 5, and 6. The vertical dashed lines show the Fermi energy at −5.44 eV. In these molecules, the HOMO is closer to the Fermi energy than the LUMO. In the calculation of the transmission through molecule 4 and 6, the hydrogen atoms of thiol linkers are removed. The percentage of the HOMO/LUMO contribution in each transmission peak is shown.

LUMO of the isolated molecule (with hydrogen atoms) are −5.92 and −2.21 eV. For molecule 5, the amine linkers will most probably stay there when the molecule is connected to the electrodes and the coupling is through the lone pair on the nitrogen atoms.[51,52] In this molecule, the HOMO energy of the isolated molecule is −6.23 eV and the LUMO is −1.93 eV, and as in molecule 4, the HOMO peak is closer to the Fermi energy than the LUMO. Therefore, the vibrational frequencies of molecules 3 and 4 should be analyzed for the neutral and oxidized states.

In the upper part of Figure 9, the vibrational spectra are shown for the cations and anions for molecule 4. In region A, the frequency of the neutral molecule is higher than that of the molecule with one electron removed. However, the changes in the frequencies of region A are not visible in the Raman spectrum (see Figure 10). We conclude that comparison of the spectra of a neutral molecule and an oxidized molecule does not show an unambiguous trend. However, if the molecule is charged by adding an extra electron, a substantial variation is observed, as shown in plot I of Figure 9 for molecule 4 (labeled as region A). Similar to molecules 1, 2, and 3, all vibrational modes (except a few modes with very low frequency) show a downward shift of the frequency upon adding an electron to the molecule, while such a uniform trend is not observed upon oxidization.

dx.doi.org/10.1021/jp307703t | J. Phys. Chem. C 2012, 116, 23120−23129

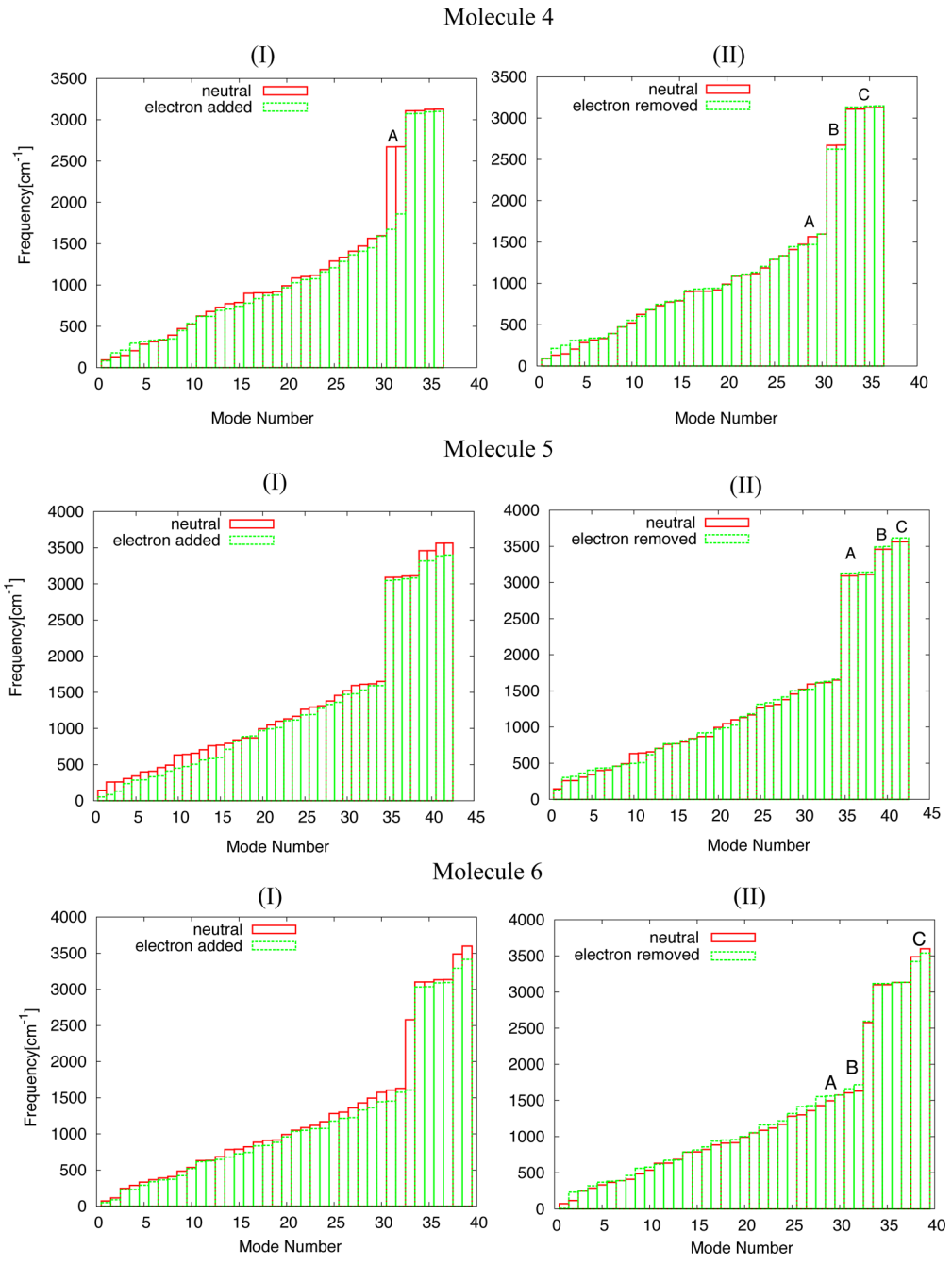

Figure 9. Molecules 4, 5, and 6: (I) The frequencies of all vibrational modes for the neutral molecule and the molecule after *adding* an electron. (II) The frequencies of all vibrational modes for the neutral molecule and the molecule with one electron *removed*. The A, B, and C regions show the modes with significant change between neutral and charged states.

For molecule 5, the Raman peaks in regions A, B, and C shift to slightly higher frequencies upon electron removal. The amine linker atoms contribute to the vibration in these regions. Mode numbers 10 and 11 show substantial frequency variation between the neutral and oxidized molecule. However, these modes do not show any strong peak in the Raman spectrum of Figure 10. Similar to the other shown molecules, for molecule 5, the comparison of vibrational frequencies of the neutral molecule and the molecule with an extra electron show that frequencies are lowered upon charging the molecule.

Molecule 6: Benzene with One Thiol Linker and One Amine Linker. Figure 8 shows the transmission of molecule 6 located between two gold electrodes. The NEGF calculations for this molecule are done with the usual sulfur−gold binding with the hydrogen atoms removed. The HOMO peak is closer to the Fermi energy than the LUMO peak, which suggests that the transport through this molecule is hole-like. Therefore, an electron should be removed from the molecule to be compared to the neutral one.

The vibrational frequencies for the neutral and oxidized molecule are shown in Figure 9. Most of the vibrational frequencies are increased upon removing an electron from the system except for the last two modes shown in region C which are related to the vibration of amine linker atoms. The corresponding Raman shifts of this molecule are shown in Figure 10.

dx.doi.org/10.1021/jp307703t | J. Phys. Chem. C 2012, 116, 23120−23129

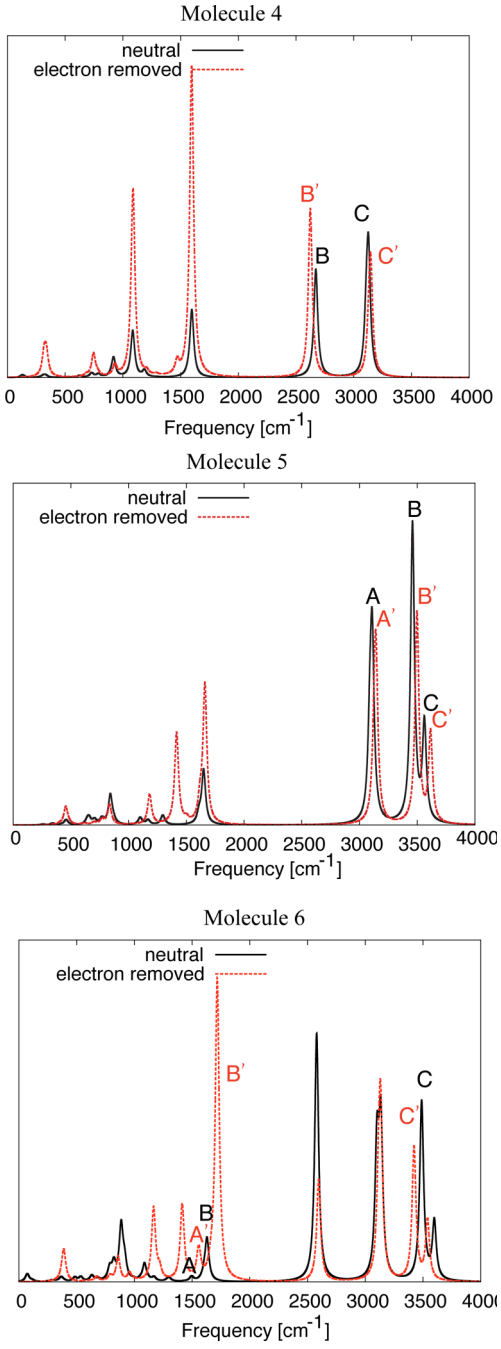

Figure 10. Molecules 4, 5, and 6: The Raman spectrum for the neutral molecule and the molecule with one electron *removed*. The peaks in regions A, B, and C for the neutral molecule are shifted to A', B', and C' when one electron is removed.

The vibrational modes of the neutral molecule are also compared to those of the molecule with an added electron. As shown in plot I of Figure 9, the frequencies are consistently lowered upon adding an electron.

From these results, we conclude that, if the frequency shifts are mostly unidirectional, transport is probably through the LUMO. If they are not, it is more likely that the HOMO is the transport orbital.

The reason that this unidirectionality is lacking in the HOMO transport is as follows: Anions are nearly always less strongly bound than neutrals. Occupation of orbitals that were empty in the neutral is occupation of (at least partially) antibonding orbitals, which lead to floppier and less well-bonded anions than in the neutral. Cations do not show such general behavior, because removing an electron from a bonding-type orbital usually gives more localized modifications in bond length and in bond strength. Therefore, we might see less consistent frequency shifts (but larger ones for some frequencies).

It should be noted that, if the bias voltage is sufficiently large to make a large electric field, the Stark effect can be observed. Ward et al.[18] observed a Stark shift of ∼15 cm^{-1} in their experiment for a three-ring oligophenylene vinylene terminated in amine functional groups. Our calculations for 4,4′-bipyridine molecule with an applied electric field of 0.5 V/nm (5 MV/cm) show that the vibrational mode frequencies can change in a similar range (up to ∼17 cm^{-1}). For the peaks that we observe shifting upon charging (regions A, B, and C), the shifts due to the Stark effect are about 10 cm^{-1}, which is an order of magnitude smaller than the predicted charge-state-induced shifts. For benzene molecules, however, the shift due to the Stark effect is very small (∼3 cm^{-1}). Therefore, the Stark shift is a gradual shift, whereas the charge-state-induced shift is sudden.

CONCLUSIONS

We have studied the possibilities for transport measurements combined with Raman spectroscopy, probing different charge states in molecular junctions. These charge states can be induced using a bias voltage provided the tunnel couplings are strongly asymmetric, but the capacitive couplings should be of the same order. We have investigated the shifts in the Raman spectra of benzene derivatives in molecules with different linkers (cyano, pyridyl, amine, and thiol groups) upon oxidation or reduction. In particular, we have compared neutral and oxidized states for 1,4-benzenedithiol, 1,4-benzenediamine, and *p*-mercaptoaniline. For the comparison between neutral and negatively charged states, we have chosen 1,4-dicyano-benzene, 1,2,4,5-tetrafluoro-3,6-dicyano-benzene, and 4,4′-bipyridine. The results predict an experimentally distinguishable difference in the Raman spectrum of the molecules between the neutral and the molecules with one electron added or removed. The frequencies of some vibrational modes change upon charging or oxidizing the molecule, and these effects appear as an observable shift in the Raman peaks corresponding to those vibrational modes. Particularly strong shifts are predicted for modes *D* of molecules 1 and 2 (Figure 7) and relatively strong shifts for modes *C* of molecules 5 and 6 (Figure 10). These frequencies are however usually related to the anchoring groups, and their frequencies therefore may vary across experiments. The most important shifts associated with internal modes of the molecules are found at region A for molecule 1, regions B and C for molecule 2, regions A and B for molecule 3, regions B and C for molecule 5, and regions A and B for molecule 6. It should be noted that the strength of our method is balanced by a few limitations such as known weakness in DFT exchange-correlation functionals and the lack of information about the exact geometry (due to the image charge effect and charge constraint). In addition, experiments can be performed in different temperatures, which may influence the results. Our results suggest that, if the frequency shifts are mostly unidirectional, transport is probably through the LUMO. If they are not, it is more likely that the HOMO is the transport orbital. We believe that these effects will lead to a better understanding of the transport process in molecular junctions.

dx.doi.org/10.1021/jp307703t | *J. Phys. Chem. C* 2012, 116, 23120−23129

AUTHOR INFORMATION

Corresponding Author

*E-mail: F.Mirjani@tudelft.nl.

Author Contributions

F.M. did the computations and drafted the manuscript. J.M.T. and M.A.R. edited the manuscript and suggested the topic.

Notes

The authors declare no competing financial interest.

ACKNOWLEDGMENTS

F.M. gratefully acknowledges the hospitality of the M.A.R. group at Northwestern University and useful discussions with B. Movaghar, R. P. van Duyne, J. S. Seldenthuis, and F. Grozema. Financial support was obtained from the EU FP7 program under the grant agreements SINGLE and ELFOS. This research was partially supported by the nonequilibrium energy research center (NERC), an Energy Frontier Research Center funded by the U.S. Department of Energy Office of Science, Office of Basic Energy Sciences under award II DE-SC0000989. M.A.R. thanks the Chem. Division of the NSF (CE1058896) for support.

REFERENCES

(1) Nitzan, A.; Ratner, M. A. *Science* **2003**, *300*, 1384.
(2) Paulsson, M.; Zahid, F.; Datta, S. In *Resistance of a molecule*; Goddard, W. A., III, Brenner, D. W., Lyshevski, S. E., Iafrate, G. J., Eds.; CRC Press: USA, 2003; Chapter in Handbook of Nanotechnology.
(3) Cuevas, J. C.; Scheer, E. *Molecular electronics, an introduction to theory and experiment*; World Scientific: Singapore, 2010.
(4) Joachim, C.; Gimzewski, J. K.; Schlittler, R. R.; Chavy, C. *Phys. Rev. Lett.* **1995**, *74*, 2102−2105.
(5) Bumm, L. A.; Arnold, J. J.; Cygan, M. T.; Dunbar, T. D.; Burgin, T. P.; Jones, L.; Allara, D. L.; Tour, J. M.; Weiss, P. S. *Science* **1996**, *271*, 1705.
(6) Stipe, B. C.; Rezaei, M. A.; Ho, W. *Science* **1998**, *280*, 1732.
(7) Moskovits, M. *Rev. Mod. Phys.* **1985**, *57*, 783−826.
(8) Campion, A.; Kambhampati, P. *Chem. Soc. Rev.* **1998**, *27*, 241−250.
(9) Nie, S. M.; Emory, S. R. *Science* **1997**, *275*, 1102.
(10) Xu, H.; Bjerneld, E. J.; Käll, M.; Börjesson, L. *Phys. Rev. Lett.* **1999**, *83*, 4357−4360.
(11) Kneipp, K.; Wang, Y.; Kneipp, H.; Perelman, L. T.; Itzkan, I.; Dasari, R. R.; Feld, M. S. *Phys. Rev. Lett.* **1997**, *78*, 1667−1670.
(12) Michaels, A. M.; Nirmal, M.; Brus, L. E. *J. Am. Chem. Soc.* **1999**, *121*, 9932−9939.
(13) Michaels, A. M.; Jiang; Brus, L. *J. Phys. Chem. B* **2000**, *104*, 11965−11971.
(14) Otto, A.; Mrozek, I.; Grabhorn, H.; Akemann, W. *J. Phys.: Condens. Matter* **1992**, *4*, 1143.
(15) Fleischmann, M.; Hendra, P.; McQuillan, A. *Chem. Phys. Lett.* **1974**, *26*, 163−166.
(16) Jeanmaire, D. L.; Duyne, R. P. V. *J. Electroanal. Chem. Interfacial Electrochem.* **1977**, *84*, 1−20.
(17) Ward, D. R.; Halas, N. J.; Ciszek, J. W.; Tour, J. M.; Wu, Y.; Nordlander, P.; Natelson, D. *Nano Lett.* **2008**, *8*, 919−924, PMID: 18237152.
(18) Ward, D. R.; Corley, D. A.; Tour, J. M.; Natelson, D. *Nat. Nanotechnol.* **2011**, *6*, 33.
(19) Liu, Z.; Ding, S.-Y.; Chen, Z.-B.; Wang, X.; Tian, J.-H.; Anema, J. R.; Zhou, X.-S.; Wu, D. Y.; Mao, B.-W.; Xu, X.; Ren, B.; Tian, Z.-Q. *Nat. Commun.* **2011**, *2*, 305.
(20) Venkataraman, L. *Nat. Nanotechnol.* **2008**, *3*, 187.
(21) Galperin, M.; Ratner, M. A.; Nitzan, A. *Nano Lett.* **2009**, *9*, 758−762, PMID: 19159246.
(22) Galperin, M.; Nitzan, A. *J. Phys. Chem. Lett.* **2011**, *2*, 2110−2113.
(23) Shamai, T.; Selzer, Y. *Chem. Soc. Rev.* **2011**, *40*, 2293−2305.
(24) Tian, J.-H.; Liu, B.; Li; Yang, Z.-L.; Ren, B.; Wu, S.-T.; Tao; Tian, Z.-Q. *J. Am. Chem. Soc.* **2006**, *128*, 14748−14749.
(25) Champagne, A. R.; Pasupathy, A. N.; Ralph, D. C. *Nano Lett.* **2005**, *5*, 305−308.
(26) Dadosh, T.; Gordin, Y.; Krahne, R.; Khivrich, I.; Mahalu, D.; Frydman, V.; Sperling, J.; Jacoby, A.; Bar-Joseph, I. *Nature* **2005**, *436*, 677.
(27) Osorio, E. A.; Bjørnholm, T.; Lehn, J.-M.; Ruben, M.; van der Zant, H. S. J. *J. Phys.: Condens. Matter* **2008**, *20*, 374121.
(28) Lambert, D. K. *Solid State Commun.* **1984**, *51*, 297−300.
(29) Shao, Y.; et al. *Phys. Chem. Chem. Phys.* **2006**, *8*, 3172−3191.
(30) Johnson, B. G.; Florián, J. *Chem. Phys. Lett.* **1995**, *247*, 120−125.
(31) Pesteil, P.; Shurvell, H. F.; Pesteil, L. *Can. J. Chem.* **1965**, *43*, 3133−3150.
(32) Lund, P.; Smardzewski, R.; Tevault, D. *Chem. Phys. Lett.* **1982**, *89*, 508−510.
(33) Mishchenko, A.; Zotti, L. A.; Vonlanthen, D.; Bürkle, M.; Pauly, F.; Cuevas, J. C.; Mayor, M.; Wandlowski, T. *J. Am. Chem. Soc.* **2011**, *133*, 184−187.
(34) Lörtscher, E.; Cho, C. J.; Mayor, M.; Tschudy, M.; Rettner, C.; Riel, H. *ChemPhysChem* **2011**, *12*, 1677−1682.
(35) Zotti, L. A.; Kirchner, T.; Cuevas, J.-C.; Pauly, F.; Huhn, T.; Scheer, E.; Erbe, A. *Small* **2010**, *6*, 1529−1535.
(36) Baheti, K.; Malen, J. A.; Doak, P.; Reddy, P.; Jang, S.-Y.; Tilley, T. D.; Majumdar, A.; Segalman, R. A. *Nano Lett.* **2008**, *8*, 715−719, PMID: 18269258.
(37) Hong, W.; Manrique, D. Z.; Moreno-García, P.; Gulcur, M.; Mishchenko, A.; Lambert, C. J.; Bryce, M. R.; Wandlowski, T. *J. Am. Chem. Soc.* **2012**, *134*, 2292−2304.
(38) Kim, Y.; Hellmuth, T. J.; Bürkle, M.; Pauly, F.; Scheer, E. *ACS Nano* **2011**, *5*, 4104−4111.
(39) Hou, S.; Zhang, J.; Li, R.; Ning, J.; Han, R.; Shen, Z.; Zhao, X.; Xue, Z.; Wu, Q. *Nanotechnology* **2005**, *16*, 239.
(40) Rauba, J. M. C.; Strange, M.; Thygesen, K. S. *Phys. Rev. B* **2008**, *78*, 165116.
(41) Kamenetska, M.; Quek, S. Y.; Whalley, A. C.; Steigerwald, M. L.; Choi, H. J.; Louie, S. G.; Nuckolls, C.; Hybertsen, M. S.; Neaton, J. B.; Venkataraman, L. *J. Am. Chem. Soc.* **2010**, *132*, 6817−6821.
(42) Reddy, P.; Jang, S.-Y.; Segalman, R. A.; Majumdar, A. *Science* **2007**, *315*, 1568.
(43) Kondo, H.; Kino, H.; Nara, J.; Ozaki, T.; Ohno, T. *Phys. Rev. B* **2006**, *73*, 235323.
(44) Ning, J.; Li, R.; Shen, X.; Qian, Z.; Hou, S.; Rocha, A. R.; Sanvito, S. *Nanotechnology* **2007**, *18*, 345203.
(45) Strange, M.; Rostgaard, C.; Häkkinen, H.; Thygesen, K. S. *Phys. Rev. B* **2011**, *83*, 115108.
(46) Mowbray, D. J.; Jones, G.; Thygesen, K. S. *J. Chem. Phys.* **2008**, *128*, 111103.
(47) ADF2010, SCM, Theoretical Chemistry, Vrije Universiteit, Amsterdam, The Netherlands, http://www.scm.com.
(48) Xue, Y.; Ratner, M. A. *Phys. Rev. B* **2004**, *69*, 085403.
(49) Kaasbjerg, K.; Flensberg, K. *Nano Lett.* **2008**, *8*, 3809−3814, PMID: 18954146.
(50) Hunt, M. R. C.; Modesti, S.; Rudolf, P.; Palmer, R. E. *Phys. Rev. B* **1995**, *51*, 10039−10047.
(51) Venkataraman, L.; Klare, J. E.; Tam, I. W.; Nuckolls, C.; Hybertsen, M. S.; Steigerwald, M. L. *Nano Lett.* **2006**, *6*, 458−462.
(52) Fagas, G.; Greer, J. C. *Nanotechnology* **2007**, *18*, 424010.
(53) Candana, M. M.; Eroğlu, S.; Özbeya, S.; Kendi, E.; Kantarci, Z. *Spectrosc. Lett.* **1999**, *32*, 35−45.
(54) Marvaud, V.; Launay, J.-P.; Joachim, C. *Chem. Phys.* **1993**, *177*, 23−30.
(55) Klein, D. R. *Organic Chemistry*; Wiley: NewYork, 2012.